Brearley, J. Alexander; Sheen, Katy L.; Naviera Garabato, Alberto C.; Smeed, David A.; Speer, Kevin G.; Thurnherr, Andreas M.; Meredith, Michael P.; Waterman, Stephanie. 2014 Deep boundary current disintegration in Drake Passage. *Geophysical Research Letters*, 41 (1). 121-127. 10.1002/2013GL058617

AGU PUBLICATIONS

Geophysical Research Letters

RESEARCH LETTER
10.1002/2013GL058617

Key Points:
- Mid-depth eddies observed east of Drake Passage
- Eddies contain fresh Pacific Deep Water
- Eddies induce transport of water properties across the ACC

Correspondence to:
J. A. Brearley,
jab5@noc.soton.ac.uk

Citation:
Brearley, J. A., K. L. Sheen, A. C. Naveira Garabato, D. A. Smeed, K. G. Speer, A. M. Thurnherr, M. P. Meredith, and S. Waterman (2014), Deep boundary current disintegration in Drake Passage, *Geophys. Res. Lett.*, *41*, 121–127, doi:10.1002/2013GL058617.

Received 7 NOV 2013
Accepted 11 DEC 2013
Accepted article online 14 DEC 2013
Published online 15 JAN 2014

Deep boundary current disintegration in Drake Passage

J. Alexander Brearley[1], Katy L. Sheen[1], Alberto C. Naveira Garabato[1], David A. Smeed[2], Kevin G. Speer[3], Andreas M. Thurnherr[4], Michael P. Meredith[5,6], and Stephanie Waterman[7]

[1]National Oceanography Centre, University of Southampton, Southampton, UK, [2]National Oceanography Centre, National Oceanography Centre, Southampton, UK, [3]Earth, Ocean and Atmospheric Science and Geophysical Fluid Dynamics Institute, Florida State University, Tallahassee, Florida, USA, [4]Lamont-Doherty Earth Observatory, Columbia University, Palisades, New York, USA, [5]British Antarctic Survey, Cambridge, UK, [6]Scottish Association for Marine Science, Oban, UK, [7]Climate Change Research Centre and ARC Centre of Excellence for Climate System Science, University of New South Wales, Sydney, New South Wales, Australia

Abstract The fate of a deep boundary current that originates in the Southeast Pacific and flows southward along the continental slope of South America is elucidated. The current transports poorly ventilated water of low salinity (a type of Pacific Deep Water, PDW), into Drake Passage. East of Drake Passage, the boundary current breaks into fresh anticyclonic eddies, nine examples of which were observed in mooring data from December 2009 to March 2012. The observed eddies appear to originate mainly from a topographic separation point close to 60°W, have typical diameters of 20–60 km and accompanying Rossby numbers of 0.1–0.3. These features are likely to be responsible for transporting PDW meridionally across the Antarctic Circumpolar Current, explaining the near homogenization of Circumpolar Deep Water properties downstream of Drake Passage. This mechanism of boundary current breakdown may constitute an important process in the Southern Ocean overturning circulation.

1. Introduction

The meridional overturning circulation (MOC) of the Southern Hemisphere oceans strongly influences the uptake of both heat and carbon from the atmosphere, and thus plays a fundamental role in global climate. A significant gap in our understanding of the Southern Ocean MOC pertains to the character and implications of the abrupt transition between the distinct dynamical regimes of the mid-depth ocean circulation to the north of and that within the Antarctic Circumpolar Current (ACC) [*Marshall and Speer*, 2012]. These intermediate waters must transit between topographically guided deep boundary currents and a strongly eddying, open channel environment as they enter the ACC, whereupon they form the Circumpolar Deep Water (CDW) that occupies much of the Southern Ocean. This process is particularly striking in Drake Passage, where topography is complex, circulation is intense, and the evolution of CDW properties along the ACC is dramatic [*Naveira Garabato et al.*, 2002].

One component of CDW originates in the South Pacific and is termed Pacific Deep Water (PDW). Analysis of a number of hydrographic sections [e.g., *Reid*, 1997; *Tsuchiya and Talley*, 1998] has shown that part of this poorly oxygenated water mass flows along the western and southern continental slopes of South America and enters the ACC in Drake Passage [*DeMets et al.*, 1990; *Tsuchiya and Talley*, 1998; *Faure and Speer*, 2012]. This deep boundary current is observed in Drake Passage, where it transports ~6 Sv ($1\ \mathrm{Sv} = 1 \times 10^6\ \mathrm{m^3\ s^{-1}}$) of a variety of PDW that is cool, fresh, depleted in oxygen, and enriched in ^{3}He and Mn relative to CDW of the same density advected from the west by the ACC [*Well et al.*, 2003; *Sudre et al.*, 2011; *Middag et al.*, 2012]. This variety of PDW has been termed Southeast Pacific Deep Slope Water [*Well et al.*, 2003]. As it is advected through Drake Passage, its pronounced low oxygen concentration signature ($< 150\ \mu\mathrm{mol\ kg^{-1}}$) centered at 2000 m depth (Figures 1a and 1b) is gradually degraded and spread along isopycnals, such that by the time it reaches the SR1b repeat hydrography line 600 km farther east (Figure 1c), the oxygen minimum has crossed the Subantarctic Front (SAF). A similar distance farther downstream, over the Falkland Plateau, where the SAF and Polar Front (PF) move to the west of South Georgia, the oxygen minimum has virtually disappeared (Figure 1d; see also *Naveira Garabato et al.* [2007]). The ^{3}He fingerprint of the water mass is, nonetheless, traceable for thousands of kilometers along the ACC [*Well et al.*, 2003].

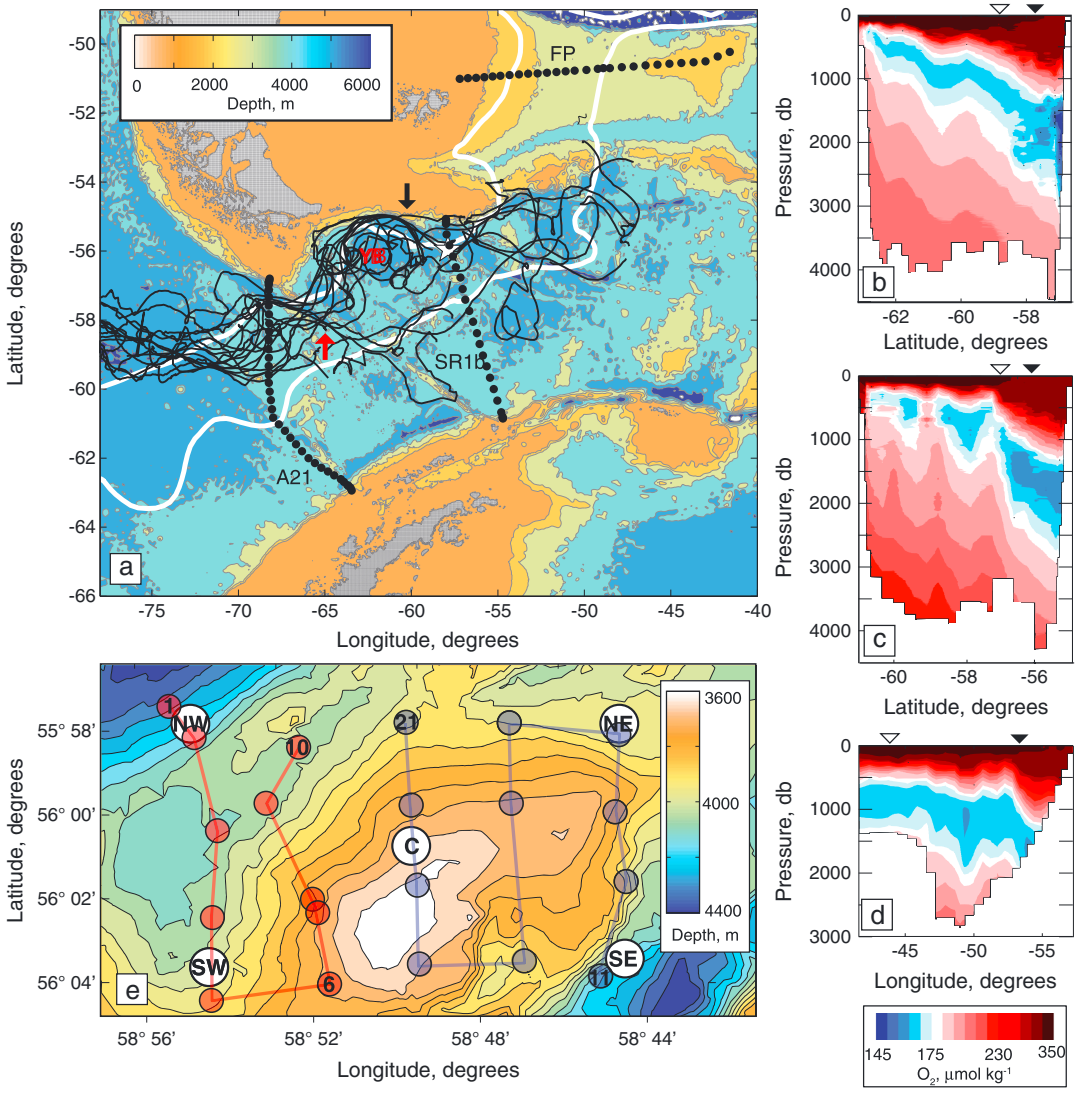

Figure 1. (a) Map of study region, showing the location of the A21 stations (from JC031), the SR1b stations (from JC031), and the Falkland Plateau stations (from JR40). Float trajectories deeper than 1500 m are marked with black lines, and the position of the mooring array and CTD stations is indicated with a star. The location of Burdwood Bank is indicated with a black arrow, the position where some float trajectories are diverted is shown with a red arrow, and Yaghan Basin is marked. Mean positions of the SAF and PF, from *Orsi et al.* [1995], are plotted. (b–d) CTD dissolved oxygen concentration (in µmol kg^{-1}) for A21, SR1b, and Falkland Plateau sections. The positions of the SAF and PF are shown with filled and open triangles. (e) Magnification of moorings (white circles) and CTD stations (colored circles), with topography shown. The western stations (in red), in particular stations 1–6, correspond to stations with the mid-depth speed maximum. The mooring array measures 10.5 km by 10.5 km.

In this paper, we analyze hydrographic observations, float trajectories, and moored time series measurements, to investigate the mechanism by which the deep boundary current containing PDW and entering the ACC in Drake Passage, disintegrates in the Scotia Sea. We present evidence that the current breaks down into mid-depth mesoscale eddies that transport PDW poleward across the ACC, inducing a homogenization of water mass properties in that density class.

2. Data

Time series of horizontal velocity (*u* and *v*), temperature (*T*), salinity (*S*), and pressure (*P*) at up to 12 levels between 400 dbar and 3600 dbar were acquired from a five-element mooring array close to 56°S, 57°50'W (Figures 1a and 1e), deployed between 12 December 2009 and 6 March 2012 as part of the Diapycnal and Isopycnal Mixing Experiment in the Southern Ocean (DIMES). The sampling interval of the measurements was

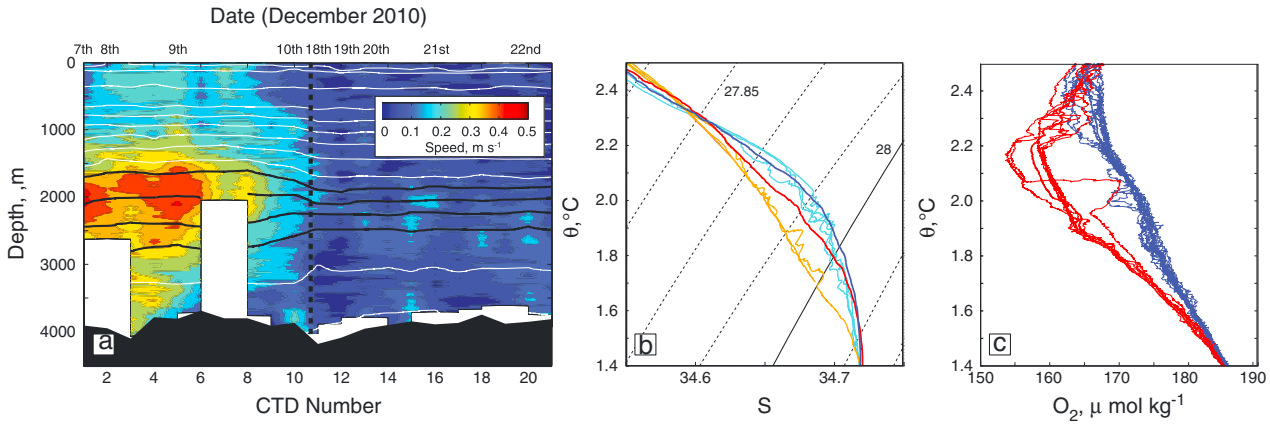

Figure 2. (a) Current speed (m s^{-1}) in color by station number for the mooring region CTDs. Neutral density surfaces at 0.05 kg m^{-3} intervals between $\gamma^n = 27.85$ and $\gamma^n = 28.00$ kg m^{-3} are marked in black. Other γ^n surfaces are contoured at 0.1 kg m^{-3} intervals in white. Times are plotted along the upper *x* axis, and the time separation between the two groups of stations is shown with a dashed line. Depths at each station are plotted with black shading; (b) The θ-*S* curves for stations 1–6 (mean, bold red), and stations 11–21 (mean, bold blue). Boundary stations north of 57.5°S on A21 are shown in orange; A21 stations between 58°S (north of the SAF) and 57.5°S are shown in cyan. γ^n surfaces at 0.05 kg m^{-3} intervals are marked; (c) θ/O_2 curves for stations 1–6 (red, mean in bold) and stations 11–21 (blue, mean in bold), with each individual profile in faint red and blue, respectively.

15–20 min, and temperature and conductivity were calibrated against ship-based conductivity-temperature-depth (CTD) data [*Brearley et al.*, 2013].

During mooring turnaround between 5 and 22 December 2010, 21 CTD and LADCP (Lowered Acoustic Doppler Current Profiler) stations were occupied by *RRS James Cook* (cruise JC054) in a grid configuration around the mooring site (Figure 1e). Salinity was calibrated using bottle samples; the resulting accuracy of *T* and *S* is 0.002°C and 0.002 [*Sheen et al.*, 2013]. CTD oxygen concentration measurements were also acquired. While these were not calibrated against bottle values, the behavior of the sensor was stable, and thus the measurements could be used comparatively to trace the low oxygen characteristic of the deep boundary current. Further CTD measurements (with calibrated oxygen) from the A21, SR1b, and Falkland Plateau lines [*Heywood and Stevens*, 2000; *McDonagh and Hamersley*, 2009] are also included in this study. These data were collected onboard *RRS James Cook* (cruise JC031, 3 February to 3 March 2009) and *RRS James Clark Ross* (cruise JR40, 15 March to 22 April 1999).

Acoustically tracked RAFOS floats, released at 105°W and 66°W in 2009 and 2010, were also used to investigate the trajectory of the PDW through Drake Passage (Figure 1a). The floats drifted at a range of depths from roughly 500 m to 2000 m. Only the deeper floats (pressures >1500 dbar) are used here. Data collection and processing are detailed in *Hancock and Speer* [2013].

3. Results

3.1. Pacific Deep Water in CTD/LADCP Data

In the A21 section, PDW is tightly constrained to the northern boundary shoreward of the Chile Trench (Figures 1a and 1b). Though the floats were not specifically deployed into this water mass, their trajectories are consistent with this flow, with most concentrated on the approximate position of the SAF just south of the boundary current. Some deeper parts of the flow appear to be diverted into the PF by a ridge (red arrow on Figure 1a), though most of the floats continue eastward along the northern boundary.

Evidence of a mid-depth signal of PDW was found in the LADCP and CTD data taken from stations 1–6 (Figure 1e) in the western part of the mooring region on 7–10 December 2010. LADCP speeds for these stations show a pronounced mid-depth intensification centered at 2000 m. By contrast, stations 11–21 do not display this feature (Figure 2a); these were collected around 11 days later (on 18–22 December). Concurrent CTD data reveal a change in stratification between those stations with and without the mid-depth maximum in speed, with a pronounced isopycnal separation between the neutral density surfaces $\gamma^n = 27.85$ and $\gamma^n = 28.00$ kg m^{-3} occurring for the first group of stations (Figure 2a) [*Jackett and McDougall*, 1997]. This is associated with a potential vorticity (PV) minimum of around 1×10^{-11} m^{-1} s^{-1} in this density range, compared with an ambient value of ~3×10^{-11} m^{-1} s^{-1}.

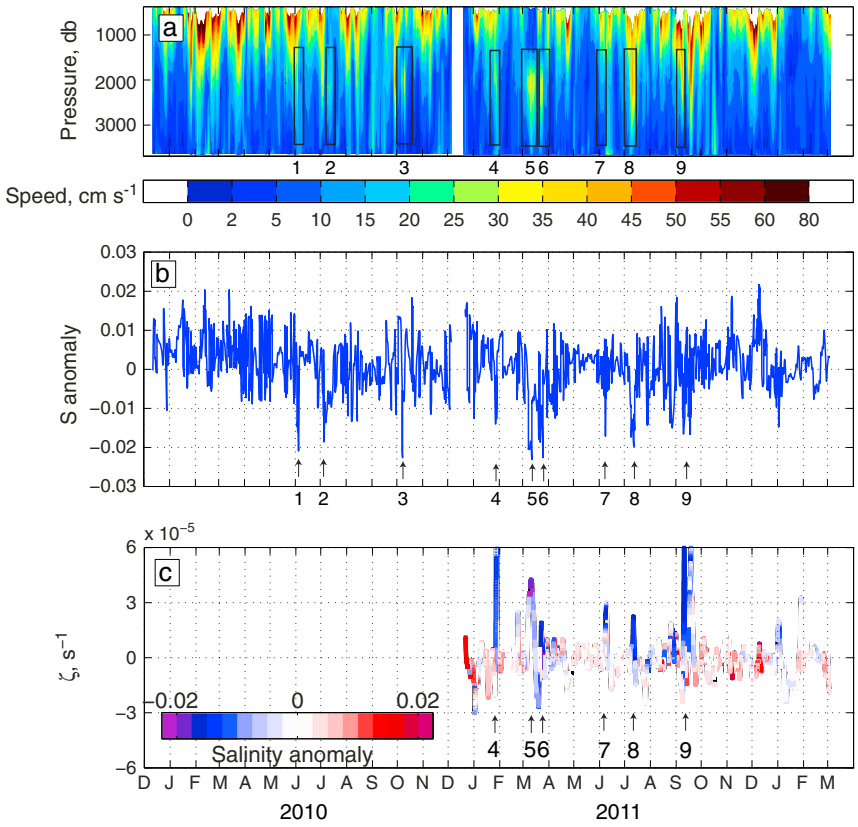

Figure 3. (a) Forty hour low-pass filtered current speed (cm s^{-1}) at the C mooring (Figure 1e). Periods of mid-depth flow intensification associated with anticyclonic eddies are indicated with black boxes. (b) Salinity anomaly (relative to mean salinity) over the θ range 1.4°C $< \theta <$ 2.1°C from a moored CTD located at a mean pressure of 2085 dbar. Periods of strong negative salinity anomaly occur alongside mid-depth flow intensification (indicated by arrows). (c) Relative vorticity ($\partial v/\partial x - \partial u/\partial y$) at a nominal pressure of 2085 dbar. This is calculated by first differences of *u* and *v* from four triangles of moorings (i.e., NW-C-NE, NE-C-SE, SE-C-SW, and SW-C-NW) and then averaged. *u* and *v* are the two components of horizontal velocity. The line is colored by salinity anomaly, and the black lines denote the edge of the contoured line.

Strong signals in both potential temperature-salinity (θ-*S*) and dissolved oxygen concentration can be found at the stations with mid-depth flow intensification, suggesting a water mass source different from the ambient CDW commonly found here in this density class. The mean θ-*S* curves for stations 1–6 (Figure 2b, in bold red) and stations 11–21 (Figure 2b, in bold blue) display a pronounced freshening (by up to 0.02) along isopycnal surfaces between $\gamma^n = 27.85$ and $\gamma^n = 28.00$ kg m^{-3} during instances when the mid-depth flow intensification is present. Moreover, stations 1–6 have lower oxygen levels at 1.6°C $< \theta <$ 2.2°C (Figure 2c), closely matching the signature of PDW from A21. Individual θ-*S* profiles from outside and inside of the boundary current in the A21 section are shown in Figure 2b. While stations 11–21 have θ-*S* properties consistent with the profiles outside the boundary current in Drake Passage, stations 1–6 are cooler, fresher, and closer in θ-*S* space to the stations within the boundary current. Furthermore, the PV minimum in stations 1–6 (1×10^{-11} m^{-1} s^{-1} in the density range $\gamma^n = 27.85$–28.00 kg m^{-3}) is also present at the same density horizon in the boundary current stations of A21 north of 57°N, while the higher PV values found in stations 11–21 are similar in magnitude to those found further to the south (not shown). Collectively, this evidence indicates that the water mass found at the mooring location in stations 1–6 is PDW sourced from the boundary current. Moreover, it is likely that the PDW observed near the mooring array is part of a mid-depth eddy structure. Below, we present further evidence endorsing this interpretation.

3.2. Eddy Events in Mooring Data

Current speeds from the C mooring are displayed in Figure 3a to assess the frequency and character of mid-depth eddy events. Nine periods of mid-depth flow intensification were observed; these are most clearly visible when the near-surface flow is weak (e.g., event 5, 3–18 March 2011), but are also seen at other times

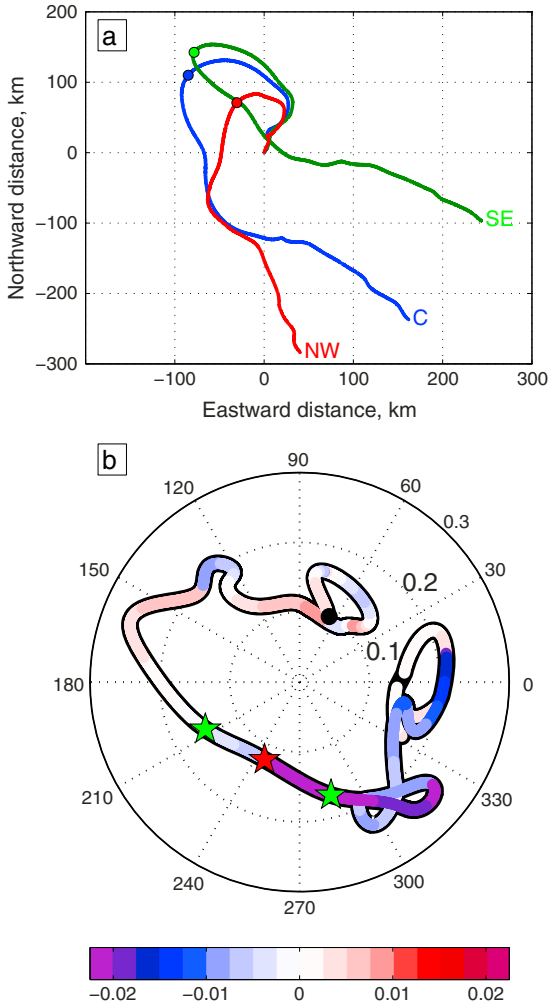

Figure 4. (a) Progressive vector diagram for three moorings between 19 February (black dot) and 31 March 2011. The day on which the anticylonic rotation is strongest is denoted by circles. (b) Hodograph for SE mooring for the same period, colored by average salinity anomaly between 1.4°C $< \theta <$ 2.1°C (as in Figure 3c). The straight line between 6 and 8 March (endpoints denoted by green stars) indicates that the mooring is intersecting the eddy core (centered on 7 March, red star). The radial axes show velocities in cm s^{-1}, and the angular coordinate shows angle in degrees from east.

(e.g., event 8, centered on 12 July 2011, when surface speed exceeds 45 cm s^{-1}). In addition, these periods are identifiable by pronounced mid-depth freshening at 1.4°C $< \theta <$ 2.1°C (Figure 3b), with the nine instances of freshest salinity in the time series being coincident with the periods of flow intensification. Particularly strong signals in salinity anomaly on θ surfaces ($>$0.02) are found in October 2010 and March 2011. Relative vorticity ζ, calculated for the second mooring deployment when five moorings were operational, is displayed in Figure 3c. The periods of freshening occur at times of strong positive ζ, suggesting advection across the region of fresh, anticyclonic lenses of PDW.

The most pronounced event (event 5), both in terms of duration and salinity anomaly, occurred between 3 and 18 March 2011, and this event is used to deduce the kinematics of these eddies. The progressive vector diagram in Figure 4a shows strong anticyclonic rotation, which impacted the entire array at this time (only three moorings are displayed for clarity). The strongest curvature is at the SE mooring, and the resultant hodograph from this location (Figure 4b) exhibits a near straight-line trajectory for 2 days duration between 6 and 8 March. This rapid transition from westward to southeastward velocity, concurrent with strong freshening, implies that the core of the eddy crossed this mooring. Peak current speeds on the edge of the feature are ~25 cm s^{-1}. Hodographs from other moorings in the array (not shown) exhibit more circular paths, implying that these moorings are affected by the eddy but are outside its core.

Table 1. Characteristics of Four Mid-Depth Anticyclonic Eddy Events That Cross the Array in Year 2 of the Deployment

Dates (Event No.)	u_a (cm s^{-1})	c (km)	Radius (km)	Ro
8–10 Sep 2011 (9)	20	43	27	0.18
12 Jul 2011 (8)	5	19	10	0.32
7 Jun 2011 (7)	14	42	22	0.15
3–18 Mar 2011 (5)	8.5	36.7	18.8	0.25

Methodology analogous to that developed by *Lilly and Rhines* [2002] was used to establish the radius of the eddy features. In their model, eddies are modeled as Rankine vortices and are composed of a region in solid body rotation with a radius, R, with a maximum azimuthal velocity, V, on the edge of the eddy core. R is estimated as $c/2 \sin(\theta/2)$, where θ is the angle formed by the chord obtained from the mooring hodograph and c is the length of the chord intersecting the eddy core. In our study, hodographs were constructed for the periods in which at least one mooring intersected the eddy core (for the interval between 21 December 2010 and 5 March 2012 as all moorings returned data during this period). The advection speed, u_a, was estimated for each event from the relative timing of the velocity maxima between the individual moorings, allowing c to be estimated. A census of these features is given in Table 1. Typical radii are 10–30 km, with azimuthal velocities being between 25 and 40 cm s^{-1}. The accompanying Rossby numbers ($Ro = 2V/Rf$, where f is the Coriolis parameter) fall between 0.1 and 0.3.

3.3. Origin and Fate of Pacific Deep Water Eddies

A key question concerns the location at which the observed eddies are generated from the boundary current. To address this, tracks of floats that pass north of 60°S in Drake Passage were analyzed (Figure 1a). While some floats separate from the boundary near 65°W (as denoted in Figure 1a, red arrow), float tracks tend to be concentrated along the northern boundary of the Yaghan Basin and then undergo detachment at a sharp change in topographic slope southwest of Burdwood Bank (Figure 1a, black arrow). From here, most floats either recirculate in the western Scotia Sea or transit eastward toward the location of the moorings, with only two of eight floats remaining on the boundary to the east of this point. One float trajectory separating from the boundary passes through the mooring array coincident with eddy event 9 in Figure 3 (centered on 8–10 September 2011).

When the boundary current disintegrates, conservation of its low PV signature relative to the ambient CDW, combined with geostrophic balance, causes the formation of eddies that are anticyclonic. In this instability process, cyclones are also generated and usually paired with the anticyclones [*Hogg and Stommel*, 1985]. However, the cyclones contain little water from the boundary current. These cyclone/anticyclone pairs, often called hetons, can then propagate away from the boundary [e.g., *Spall et al.*, 2008]. Although data are limited, there is some evidence from the moorings (Figure 3c) that periods of cyclonic rotation sometimes occur at points close in time to the large anticyclones (e.g., the negative ζ signal immediately preceding event 9, Figure 3c). Furthermore, water in these cyclones does not possess the low salinity characteristic of the PDW eddies, lending support to this proposed mechanism. When combined with the large-scale eastward flow of the region, the anticyclonic eddies can therefore transport PDW poleward across the ACC, which may induce a rapid homogenization of water mass properties downstream of Drake Passage.

4. Conclusions

In this study, mid-depth anticyclonic eddies containing PDW have been documented 450 km to the east of Drake Passage. Over a 26 month record, nine eddies were observed. These were centered at 2000 m depth and on $\gamma^n = 27.9$ kg m^{-3} and had low-salinity cores, radii of 10–30 km, and Rossby numbers of 0.1 to 0.3. A major separation point from the boundary is observed in this study near Burdwood Bank; this location was previously identified as the site where the deep cyclonic circulation of the Yaghan Basin detaches from the boundary [*Ferrari et al.*, 2012]. That study also observed the generation of an anticyclonic eddy along the northern boundary upstream of Burdwood Bank, which may be a precursor to detachment.

While PDW in Drake Passage is confined to the area north of the PF, by 35°W it is equally distributed between waters north and south of the PF [*Well et al.*, 2003]. This study suggests that mid-depth eddies generated by a topographically induced instability may provide an effective route by which PDW crosses the ACC in the Scotia Sea. While it is not possible to ascertain the poleward penetration of the eddies (as the moorings were

located north of the SAF for most of the record), the eddies were observed at a wide range of dynamic height values, suggesting that they are not confined to a narrow zone at the northern edge of the ACC. Furthermore, the work underscores the importance of Drake Passage as a site of intense cross-stream transfers, erasing the strong property anomalies of a deep boundary current. The instability process on the northern boundary of the passage provides a mechanism by which mid-depth water masses that ultimately form the CDW are transported between the distinct dynamical regimes of the subtropics and the ACC.

Acknowledgments

We thank E. McDonagh and G. Evans for JC031 data collection and preparation. Funding for DIMES was provided by Natural Environment Research Council grants NE/E007058/1 and NE/E005667/1 and National Science Foundation grants OCE-1231803, OCE-0927583, and OCE-1030309.

The Editor thanks Helen Phillips and an anonymous reviewer for their assistance in evaluating this paper.

References

Brearley, J. A., K. L. Sheen, A. C. Naveira Garabato, D. A. Smeed, and S. Waterman (2013), Eddy-induced modulation of turbulent dissipation over rough topography in the Southern Ocean, *J. Phys. Oceanogr.*, *43*, 2288–2308.

DeMets, C., R. G. Gordon, D. F. Argus, and S. Stein (1990), Current plate motions, *Geophys. J. Int.*, *101*, 425–478.

Faure, V., and K. Speer (2012), Deep circulation in the eastern South Pacific Ocean, *J. Mar. Res.*, *70*, 748–778.

Ferrari, R., C. Provost, A. Renault, N. Sennéchael, N. Barré, Y.-H. Park, and J. H. Lee (2012), Circulation in Drake Passage revisited using new current time series and satellite altimetry: 1. The Yaghan Basin, *J. Geophys. Res.*, *117*, C12024, doi:10.1029/2012JC008264.

Hancock, C., and K. Speer (2013), Diapycnal and Isopycnal Mixing Experiment in the Southern Ocean, RAFOS float data report, February 2009–February 2012, Marine Field Group, *Report 2013-1*.

Heywood, K. J., and D. P. Stevens (Eds.) (2000), *RRS James Clark Ross Cruise 40, 15th March–22nd April 1999. Antarctic Large-Scale Box Analysis and the Role of the Scotia Sea*, Cruise Report No. 6, UEA, Norwich, U.K.

Hogg, N. G., and H. M. Stommel (1985), The heton, an elementary interaction between discrete baroclinic geostrophic vortices, and its implications concerning eddy heat-flow, *Proc. R. Soc. A*, *397*, 1–20, doi:10.1098/rspa.1985.0001.

Jackett, D. R., and T. J. McDougall (1997), A neutral density variable for the world's oceans, *J. Phys. Oceanogr.*, *27*, 237–263.

Lilly, J. M., and P. B. Rhines (2002), Coherent eddies in the Labrador Sea observed from a mooring, *J. Phys. Oceanogr.*, *22*, 595–598.

Marshall, J., and K. Speer (2012), Closure of the meridional overturning circulation through Southern Ocean upwelling, *Nat. Geosci.*, *5*, 171–180.

McDonagh, E. L., and D. R. C. Hamersley (Eds.) (2009), *RRS James Cook Cruise JC031, 03 Feb-03 Mar 2009. Hydrographic Sections of Drake Passage*, 170 pp., National Oceanography Centre Southampton Cruise Report, (39), National Oceanography Centre, Southampton, U.K.

Middag, R., H. J. W. de Baar, P. Laan, and O. Huhn (2012), The effects of continental margins and water mass circulation on the distribution of dissolved aluminum and manganese in Drake Passage, *J. Geophys. Res.*, *117*, C01019, doi:10.1029/2011JC007434.

Naveira Garabato, A. C., K. J. Heywood, and D. P. Stevens (2002), Modification and pathways of Southern Ocean deep waters in the Scotia Sea, *Deep Sea Res., Part I*, *49*, 681–705.

Naveira Garabato, A. C., D. P. Stevens, A. J. Watson, and W. Roether (2007), Short-circuiting of the overturning circulation in the Antarctic Circumpolar Current, *Nature*, *447*, 194–197, doi:10.1038/nature05832.

Orsi, A. H., T. Whitworth III, D. Worth, and W. D. Nowlin Jr. (1995), On the meridional extent and fronts of the Antarctic Circumpolar Current, *Deep Sea Res., Part I*, *42*, 641–673.

Reid, J. L. (1997), On the total geostrophic circulation of the Pacific Ocean: Flow patterns, tracers and transports, *Prog. Oceanogr.*, *39*, 263–352.

Sheen, K. L., et al. (2013), Rates and mechanisms of turbulent dissipation and mixing in the Southern Ocean: Results from the DIMES experiment, *J. Geophys. Res. Oceans*, *118*, 2774–2792, doi:10.1002/jgrc.20217.

Spall, M. A., R. S. Pickart, P. A. Fratantoni, and A. J. Plueddemann (2008), Western Arctic shelfbreak eddies: Formation and transport, *J. Phys. Oceanogr.*, *38*, 1644–1668.

Sudre, J., V. Garcon, C. Provost, N. Sennéchael, O. Haun, and M. Lacombe (2011), Short-term variations of deep water masses in Drake Passage revealed by a multiparametric analysis of the ANT-XXIII/3 bottle data, *Deep Sea Res., Part II*, *58*, 2592–2612.

Tsuchiya, M., and L. D. Talley (1998), A Pacific hydrographic section at 88°W: Water-property distribution, *J. Geophys. Res.*, *103*, 12,899–12,918.

Well, R., W. Roether, and D. P. Stevens (2003), An additional deep water mass in Drake Passage as revealed by ^{3}He data, *Deep Sea Res., Part I*, *50*, 1079–1098.